Wavelet analysis of a Gaussian Kolmogorov signal

Wavelet analysis of a Gaussian Kolmogorov signal

M Vergassola†, R Benzi‡, L Biferale‡ and D Pisarenko†§

† CNRS, Observatoire de Nice, BP 229, 06304 Nice Cedex 4, France
‡ Dipartimento di Fisica, Università 'Tor Vergata', Via E Carnevale, I-00173, Rome, Italy

Abstract. Several attempts have been made recently to use wavelets transforms for extracting histograms of scaling exponents from experimental turbulence data. Similar techniques are here applied to a Gaussian signal having a Kolmogorov $\frac{5}{3}$ energy spectrum. This is an instance of the class of *fractional Brownian motions*, having scaling exponent $\frac{1}{3}$ almost everywhere. For the Gaussian signal, a spurious non-trivial histogram is obtained by applying a Mexican hat wavelet transform analysis. On the other hand, we show that the use of complex wavelets and, even more so, the application of an *optimal wavelet transform* method strongly reduce the spurious fluctuations observed in the processing of the Gaussian signal.

In Kolmogorov's theory of fully developed turbulence [1], global scale invariance in the inertial range is assumed: the statistics of the longitudinal velocity increments $\delta_\ell v \equiv v(x + \ell) - v(x)$ is invariant under the scaling transformation

$$\delta_{\lambda\ell} v \to \lambda^h \delta_\ell v \tag{1}$$

where h is the scaling exponent. In order to select the value of h, the relation proved by Kolmogorov himself [2]

$$\langle (\delta_\ell v)^3 \rangle = -\frac{4}{5}\epsilon\ell \tag{2}$$

is used (here, ϵ is the average rate of energy dissipation). If ζ_p denotes the scaling exponent of the structure functions

$$\langle \delta_\ell v^p \rangle \sim \ell^{\zeta_p} \tag{3}$$

the prediction $\zeta_p = p/3$ immediately follows. Actually, the experimental measurements performed up to now [3] show that the ζ_p function is not linear, bending downwards for high values of p. In order to provide an interpretation for these results, the multifractal model [4] was proposed. Global scale invariance is replaced by local scale invariance. The scaling exponent is then a function of the point and the set of points having the same singularity exponent h is a fractal set having dimension $D(h)$. An interpretation for an arbitrary ζ_p function in terms of another arbitrary function $D(h)$ can be provided. It is then natural to search for new independent tests of the model.

A first possible method is to study *global* properties. Indeed, it has been shown [5] that the multifractal model predicts a new form of universality of the energy spectrum with respect to the Reynolds number in the near-dissipative range of scales. One other possibility

§ Permanent address: International Institute of Mathematical Geophysics, Academy of Sciences, 79-2 Warshavskoe sh, 113556 Moscow, USSR.

in the same spirit is the study of the moments of the energy dissipation relating the local energy dissipation and the velocity increments trough a relation proposed by Kolmogorov in 1962 [6]. In both cases, the analysis of the experimental data does not contradict the multifractal model [7–9].

An alternative method is to study *local* properties. The natural tool for this kind of approach is represented by wavelet transforms. In the context of dynamical systems this technique is able to reveal the successive fractal branchings characteristic of self-similar invariant measures on strange attractors [10]. Due to their ability to detect singularities, wavelet transforms were then applied to the analysis of turbulence data [11]. In the latter case bifurcations are also observed, suggestive of some form of energy cascade. In a subsequent work [12] it was actually shown that bifurcations are already observed in the case of a Gaussian process. In this case, branchings have no dynamical meaning because they are due to a kinematic level-crossing phenomenon. In the same work, a histogram of scaling exponents was also obtained. Scaling exponents were calculated by making a least-squares fit of the plot of the logarithm of the absolute value of the wavelet transform versus the logarithm of the scale over the region corresponding to the inertial range. The analysing wavelet used was the Mexican hat. The measured histogram show a considerable scatter around the value $\frac{1}{3}$ including negative values. It was then suggested that the histogram reflected the existence of various scaling exponents.

We also mention that wavelet transforms have also been used as a *global* processing technique allowing one to improve the measurements based on structure functions [13].

In this paper we shall first perform the wavelet analysis of a Gaussian globally self-similar signal having a Kolmogorov $\frac{5}{3}$ energy spectrum. A single exponent $\frac{1}{3}$ is then present. Actually, when the signal is processed as in [12], the same scatter in the histogram of the scaling exponents is found. The phenomenon of spurious exponents is due to finite inertial range effects. We then show that the presence of spurious exponents can be strongly reduced by using complex wavelets and taking advantage of the freedom in the choice of the analysing wavelet to choose an optimal wavelet transform, as proposed in [14]. Finally, these techniques are applied to the same turbulence data used in [12]. The scatter of the measured exponents around the value $\frac{1}{3}$ is strongly reduced, thus confirming the spurious nature of the histogram shown in [12].

Let us briefly recall the basic properties of wavelet transforms. The wavelet transform at the point x of a signal $v(x)$ is defined as

$$T_g(a, x) = \int v(y) g\left(\frac{x - y}{a}\right) \frac{\mathrm{d}y}{a} .$$ (4)

The parameter $a > 0$ will be referred to as the scale and the analysing wavelet $g(\cdot)$ satisfies the zero-average constraint

$$\int g(x) \, \mathrm{d}x = 0 .$$ (5)

A wavelet that is commonly used is the mexican hat: $g(x) = -\mathrm{d}^2 \exp(-x^2/2)/\mathrm{d}x^2$. The convolution (4) can be regarded as a mathematical microscope where a and g govern the magnification and the kind of optics. The importance of wavelet transforms is essentially due to their capability of revealing scaling laws. In fact, it can be proved [15] that when the increments $|v(x + \rho) - v(x)|$ of the original signal behave as a power law ρ^h, the corresponding wavelet transform will behave as a^h. How the latter relation should be recasted in the case of globally self-similar stochastic processes like K41 turbulence or the class of fractional Brownian motions [17] has been studied in [16]. It can be shown that the wavelet transform has a scaling part, but also a noisy contribution. If the logarithm
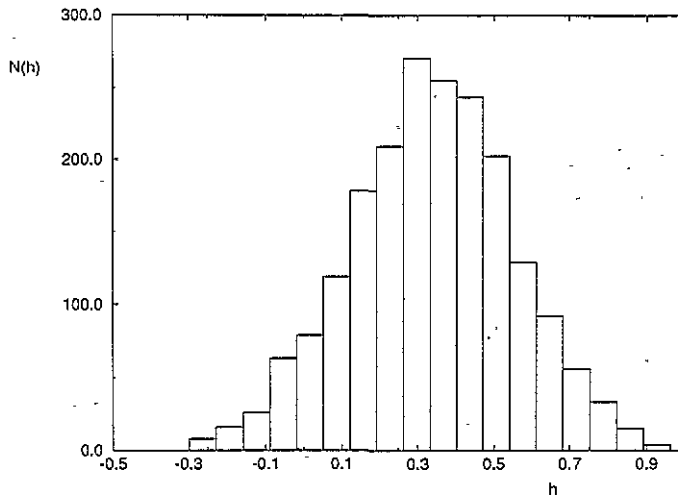
Figure 1. The histogram of scaling exponents for fractional Brownian signal of exponent $\frac{1}{3}$. The quantity $N(h)$ denotes the number of points where the *measured* scaling exponent is h. The ratio between the maximal and the minimal scale used for the fit is 500. The wavelet used is the Mexican hat.

of the absolute value of the wavelet transform is plotted versus the logarithm of the scale a, stationary fluctuations are superposed on the straight line corresponding to the scaling exponent. In particular, strong negative fluctuations are expected due to the fact that the expectation value of the wavelet transform is zero. When a finite range of scales is available, the determination of the scaling exponent by a least-squares fit can then be very noisy.

In order to gain a better understanding of the results obtained in turbulence, we have processed a fractional Brownian motion of exponent $\frac{1}{3}$ in the same way as in [12]. The signal is generated through its Fourier transform. The analysing wavelet used is the Mexican hat. The range of scales used to extract scaling exponents is chosen in such a way that the ratio between the maximum and the minimum scale is 500, a value comparable to the width of the inertial range in turbulence data. The scaling exponents are estimated in 2000 points out of 200 000 data points by a least-squares fit of the logarithm of the absolute value of the wavelet transform versus the logarithm of the scale. The resulting histogram is shown in figure 1. The most striking feature is the considerable spurious scatter of the measured exponents around the true value $\frac{1}{3}$. The dispersion around the mean value 0.34 is 0.21. Figure 1 looks very similar to the histogram obtained by analysing turbulence data (cf figure 4). The comparison leads to invalidate the interpretation of the scatter as an indication of the existence of various scaling exponents which was proposed in [12].

In order to have meaningful local information about the kind of self-similarity (if any) involved in turbulence a more reliable way of estimating scaling exponents must be sought. Hereafter, we shall discuss complex wavelets and the optimal wavelet technique. An alternative method is that of wavelet transform modulus maxima, introduced in [18].

A first way of reducing fluctuations is through the use of complex wavelets [19]. Practically, the Fourier transform $\hat{g}_C(k)$ of the complex wavelet $g_C(\cdot)$ is obtained from the Fourier transform $\hat{g}(k)$ of an usual real wavelet $g(\cdot)$ by setting the negative wavenumbers

to zero

$$\hat{g}_C(k) = \begin{cases} g(k) & \text{if } k > 0 \\ 0 & \text{if } k \leqslant 0. \end{cases} \tag{6}$$

Let us now denote by $|T_{gc}|$ the modulus of the complex wavelet transform T_{gc} obtained by using g_C as analysing wavelet and by T_g the wavelet transform using g. The reduction of noise is due to the fact that sine and cosine, and then the real and the imaginary part of the wavelet transform, are not in phase: it is likely that when the real part is near to zero the imaginary part will not and conversely. The zero level crossings of $|T_{gc}|$ are then strongly reduced with respect to those of T_g. In order to have a quantitative confirmation, we have studied analytically the wavelet transform of a Gaussian process . The results concerning the second- and third-order moments are as follows:

$$\frac{\sigma^2(|T_{gc}|^2)}{(\langle|T_{gc}|^2\rangle)^2} = 1 \qquad \frac{\langle(|T_{gc}|^2 - <|T_{gc}|^2\rangle)^3\rangle}{(\langle|T_{gc}|^2\rangle)^3} = 2$$

$$\frac{\sigma^2(T_g^2)}{(\langle T_g^2\rangle)^2} = 2 \qquad \frac{\langle(T_g^2 - \langle T_g^2\rangle)^3\rangle}{(\langle T_g^2\rangle)^3} = 8 \tag{7}$$

and the analysis of higher order moments shows that the reduction in the relative fluctuations increases with the order of the moment. The previous qualitative arguments concerning the reduction of noise produced by the use of complex wavelets are then well supported by (7).

The second way we have used to reduce fluctuations is the optimal wavelet technique, suggested in [14]. Let us briefly recall the proposal. As discussed in [16], the statistical properties of the noisy part of the wavelet transform depend on the analysing wavelet, while the scaling exponent does not. It is thus reasonable to search for the analysing wavelet that minimizes fluctuations. Such a wavelet can be constructed as a linear combination of several analysing wavelets. The weights of these wavelets are then subject to an optimization procedure that maximizes the correlation coefficient of the least-squares fit.

Specifically, let $H_p(\cdot)$ denote the Hermite function of order p and let us decompose the analysing wavelet $g(\cdot)$ as

$$g(x, \{c_p\}) = \sum_{p=1}^{M} c_p H_p(x) \exp(-x^2/2) . \tag{8}$$

For the sake of clarity, the parametric dependence of $g(\cdot)$ on the set of random coefficients c_p's has been explicitly indicated. The choice of the maximum order M will be discussed below. The decomposition of the wavelet transform corresponding to (8) is

$$T_g(a, \{c_p\}) = \sum_{p=1}^{M} c_p T_{H_p}(a) . \tag{9}$$

Because we are interested in the scaling of the wavelet transform, it is clear that the free parameters are the $M - 1$ independent ratios of the coefficients c_p. For example, the normalization condition $\sum_{p=1}^{M} c_p = 1$ can be imposed.

Practically, we used the simplest optimization technique consisting in a series of length N of Monte Carlo trials. For each choice of the set $\{c_p, \ p = 1, \ldots, M\}$ the correlation coefficient $K(\{c_p\})$ of $\log |T_g(a, \{c_p\})|$ with respect to $\log(a)$ is calculated. Between the N possible choices, the optimal wavelet g^{opt} is provided by the set of coefficients such that the maximum K is obtained. The scaling exponent is then estimated by a least-squares fit.

Concerning the choice of the maximum order M in (8), one has to be aware that when the order p is increased the Hermite functions become less and less local. As a consequence,
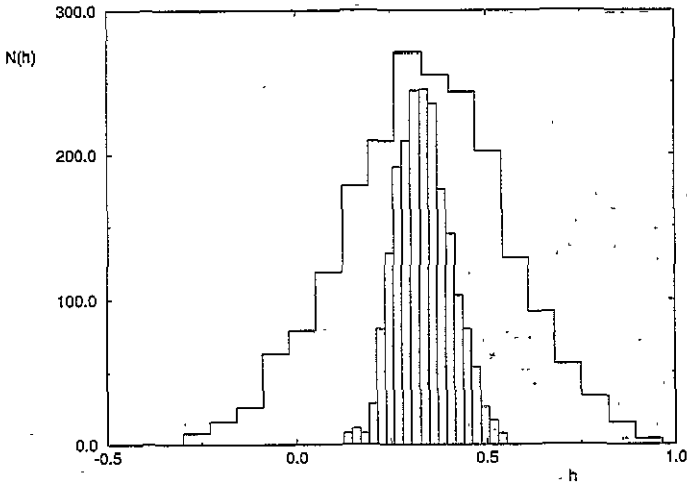
Figure 2. The histogram (small) of scaling exponents obtained by the optimal wavelet technique with the same conditions as in figure 1, superposed on the histogram of figure 1 (large) for comparison.
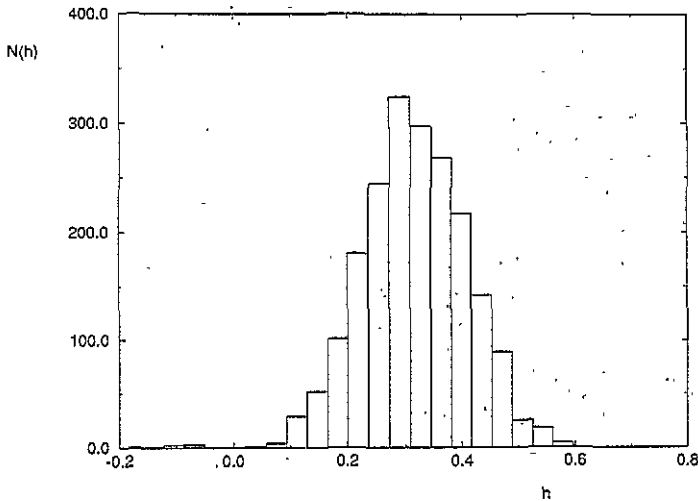

Figure 3. The histogram of exponents of the Modane turbulent signal measured by the optimal wavelet technique. The ratio between the maximal and the minimal scale used for the fit is 500. Three wavelets are used for the optimization.

with a finite inertial range, in order to avoid a mixing between the contributions coming from the inertial range and the non-scaling scale regions, one cannot increase M at will. We remark that by using the optimal wavelet technique the analysing wavelet is not the same at all the points x where the exponent is calculated. This does not constitute a problem but, on the contrary, is in the spirit of wavelet transforms which focus on local properties.

In order to test the validity of the techniques previously outlined, we have analysed the same signal as that in figure 1. In the optimization procedure, three wavelets are used and the number of Monte Carlo trials is 400 at each point. The resulting histogram is shown
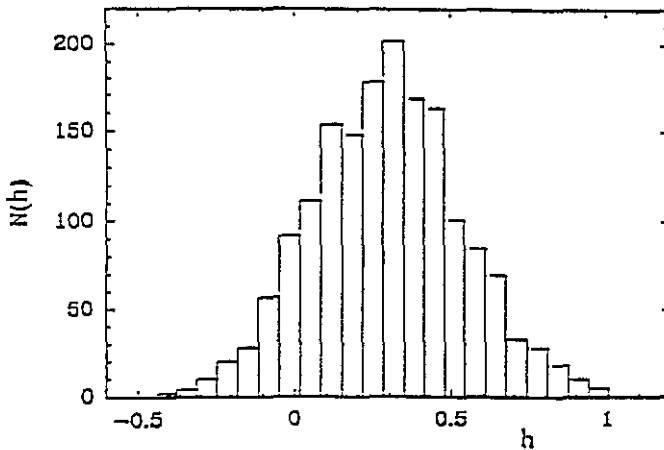
Figure 4. Histogram of scaling exponents of the Modane turbulent signal taken from [12]. The fact that the hystogram is much broader than in figure 3 is an artefact.

in figure 2 superposed on the histogram of figure 1 to make the comparison easier. The reduction in the spurious scatter is remarkable. The average value is 0.33, the standard deviation is 0.09 and the average correlation coefficient of the least-squares fits used to evaluate the scaling exponents is 0.7.

As a final check we have applied the optimized wavelet technique to the same Modane turbulence data used in [12] (for more details about these data the reader is referred to [12] and references therein). The resulting histogram is shown in figure 3. The reduction of the scatter with respect to the histogram in [12] (reproduced here as figure 4) confirms the fact that the latter does not reflect a real distribution of exponents in turbulent signals.

In our opinion, the results contained in this paper are related to the nature of self-similarity of turbulent signals. For a pure multiplicative process, there is no local scaling exponent but by the large-deviation theory one can show that the moments are indeed power laws. Recently, the same idea has been used in [20] to produce a signal which is self-similar in a statistical sense but has no scaling exponent at a single point. The application of wavelet techniques to such a signal produces the same results as for turbulence data. When one uses *global* techniques, as in [13] or such as structure functions, the signal appears self-similar with well-defined scaling exponents. If *local* techniques, like those discussed in this paper, are used, the most probable exponent is selected with a small variance due to finite-size effects. We then argue that the scaling exponents and the singularity spectrum $D(h)$ originally proposed in [4] must be interpreted in the sense of multiplicative processes.

Acknowledgments

References

[1] Kolmogorov A N 1941 *Dokl. Akad. Nauk SSSR* **30** 301

[2] Landau L D and Lifshitz E M 1987 *Fluid Mechanics* (Oxford: Pergamon) 2nd edn
[3] Anselmet F, Gagne Y, Hopfinger E J and Antonia R A 1984 *J. Fluid Mech.* **140** 63
[4] Parisi G and Frisch U 1983 *Turbulence and Predictability in Geophysical Fluid Dynamics (Proc. Int. School of Physics 'E Fermi', Varenna, Italy)* ed M Ghil, R Benzi and G Parisi, p 84
[5] Frisch U and Vergassola M 1991 *Europhys. Lett.* **14** 439
[6] Kolmogorov A N 1962 *J. Fluid Mech.* **13** 82
[7] Benzi R, Paladin G, Parisi G and Vulpiani A 1984 *J. Phys. A: Math. Gen.* **17** 3521
[8] Gagne Y and Castaing B 1991 *C.R. Acad. Sci.* **312** 414
[9] Meneveau C and Sreenivasan K R 1991 *J. Fluid Mech.* **224** 429
[10] Arnéodo A, Grasseau G and Holschneider M 1988 *Phys. Rev. Lett.* **61** 2287
[11] Argoul F, Arnéodo A, Grasseau G, Gagne Y, Hopfinger E J and Frisch U 1989 *Nature* **338** 51
[12] Bacry E, Arnéodo A, Frisch U, Gagne Y and Hopfinger E J 1990 *Turbulence and Coherent Structures* ed O Métais and M Lesieur (Dordrecht: Kluwer) p 203
[13] Muzy J F, Bacry E and Arnéodo A 1991 *Phys. Rev. Lett.* **67** 3515
[14] Benzi R and Vergassola M 1991 *Fluid Dyn. Res.* **8** 117
[15] Holschneider M 1988 *J. Stat. Phys.* **50** 963
[16] Vergassola M and Frisch U 1991 *Physica* **54D** 58
[17] Mandelbrot B 1965 *C.R. Acad. Sci.* **260** 3274
[18] Mallat S and Huang W L 1992 *IEEE Trans. Inf. Theor.* **38** 617
[19] Farge M 1991 private communication
[20] Benzi R, Biferale L, Crisanti A, Paladin G, Vergassola M and Vulpiani A 1993 *Physica* **65D** 352